

Pilot Reuse Strategy Maximizing the Weighted-Sum-Rate in Massive MIMO Systems

Jy-yong Sohn, Sung Whan Yoon, *Student Member, IEEE*, and Jaekyun Moon, *Fellow, IEEE*

Abstract—Pilot reuse in multi-cell massive multi-input multi-output (MIMO) system is investigated where user groups with different priorities exist. Recent investigation on pilot reuse has revealed that when the ratio of the coherent time interval to the number of users is reasonably high, it is beneficial not to fully reuse pilots from interfering cells. This work finds the optimum pilot assignment strategy that would maximize the weighted sum rate (WSR) given the user groups with different priorities. A closed-form solution for the optimal pilot assignment is derived and is shown to make intuitive sense. Performance comparison shows that under wide range of channel conditions, the optimal pilot assignment that uses extra set of pilots achieves better WSR performance than conventional full pilot reuse.

Index Terms—Massive MIMO, Multi-cell MIMO, Pilot contamination, Pilot assignment, Pilot reuse, Channel estimation, Weighted-Sum-Rate maximization

I. INTRODUCTION

Deployment of multiple antennas at the transmitter and the receiver, collectively known as MIMO technology, has been instrumental in improving link reliability as well as throughput of modern wireless communication systems. Under the multi-user MIMO setting, the latest development has been the use of an exceedingly large number of antennas at base stations (BSs) compared to the number of user terminals (UTs) served by each BS. Under this "massive" MIMO setup, assuming time-division-duplex (TDD) operation with uplink pilot training for channel state information (CSI) acquisition, the effect of fast-fading coefficients and uncorrelated noise disappear as the number of BS antennas increases without bound [1], [2]. Massive MIMO is considered as a promising technique in 5G communication systems, which has a potential of increasing spectral and energy efficiency significantly with simple signal processing [3]–[5]. The only factor that limits the achievable rate of massive MIMO system is the pilot contamination, which arises due to the reuse of the same pilot set among interfering cells. The pilot reuse causes the channel estimator error at each BS, where precoding scheme is also contaminated by inaccurate channel estimation. This phenomenon degrades the achievable rate of a massive MIMO system even when M , the number of BS antennas, tends to infinity; this remains as a fundamental issue in realizing massive MIMO.

Various researchers have suggested ways to mitigate pilot contamination effect, which are well summarized in [6]. A pilot transmission protocol which reduces pilot contamination

is suggested in [7]. They considered a time-shifted pilot transmission, which systematically avoids collision between non-orthogonal pilot signals. However, central control is required for this scheme, and back-haul overload remains as an issue. Realizing that inaccurate channel estimation is the fundamental reason for pilot contamination, some researchers have focused on effective channel estimation methods for reducing pilot contamination. Exploitation of the angle-of-arrival (AoA) information in channel estimation is considered [8], which achieves interference-free channel estimation and effectively eliminates pilot contamination when the number of antennas increases without bound. However, the channel estimation method of [8] uses 2^{nd} order statistics for the channels associated with pilot-sharing users in different cells, requiring inter-cell cooperation via a back-haul network. Under the assumption of imperfect CSI, another researchers investigated uplink/downlink signal processing schemes to mitigate pilot contamination [9]–[11]. A precoding method called pilot contamination precoding (PCP) is suggested to reduce pilot contamination [10]. This method utilizes slow fading coefficient information for entire cells, and cooperation between BSs is required. Multi-cell MMSE detectors are considered in several literatures [11]–[14], but interference due to pilot contamination cannot be perfectly eliminated. Moreover, most of these works rarely consider the potential of pilot allocation in reducing pilot contamination.

Some recent works shed light on appropriate pilot allocation as a candidate to tackle pilot contamination. There are three types of pilot allocation: one is to allocate orthogonal pilots within a cell assuming full pilot reuse among different cells [8], [15], [16], another is reusing a single pilot sequence among users within a cell, while users in different cells employ orthogonal pilots [17], and the other is finding the pilot reuse rule among different cells whereas all users within a cell are guaranteed to be assigned orthogonal pilots [11], [18]–[20].

A coordination-based pilot allocation rule is suggested in [8], which shapes the covariance matrix in order to achieve interference-free channel estimation and eliminate pilot contamination. However, back-haul overload is required to apply the suggested pilot allocation method. Another coordination-based pilot allocation in [15] utilizes slow-fading coefficient information, where the pilot with the least inter-cell interference is assigned to the user with the worst channel quality. The optimal allocation rule of resources (transmit power, the number of BS antennas, and the pilot training signal) which maximizes the spectral efficiency is considered in [16]. Cooperation among BSs is assumed in this optimization, where each BS transmits the path-loss coefficients information to other

Manuscript received December 1, 2016; accepted March 6, 2017. The authors are with the School of Electrical Engineering, Korea Advanced Institute of Science and Technology, Daejeon, 305-701, Republic of Korea (e-mail: jysohn1108@kaist.ac.kr, shyoon8@kaist.ac.kr, jmoon@kaist.edu).

interfering cells. All these works show that appropriate pilot assignment is important in reducing pilot contamination, but they all suggest coordination-based solutions which have implementation issues. On the other hand, reusing the same pilot within a cell is considered in [17], whereas interfering cells have orthogonal pilots. The pilot reuse within a cell causes intra-cell interference, which is eliminated by the downlink precoding scheme suggested in the same paper. However, the interference is fully eliminated only when the number of BS antennas is infinite and the equivalent channel is invertible; the solution for a general setting still remains as an open problem.

Unlike conventional full pilot reuse, some researchers considered less aggressive pilot reuse scheme as a candidate for reducing pilot contamination. Simulation results in [11], [18], [19] showed that less aggressive pilot reuse can increase spectral efficiency in some practical scenarios, but the approaches are not based on a closed-form solution, which does not offer useful insights into the trade-off between increased channel estimation accuracy and decreased data transmission time. Perhaps [20] is the first paper which observed and mathematically analyzed the trade-off when less aggressive pilot reuse is applied. In [20], the present authors analyzed the potential of using more pilots than K , the number of UTs in a BS, to mitigate pilot contamination and increase the achievable rate. Based on lattice-based hexagonal cell partitioning, they formulated the relationship between normalized coherence time and the optimal number of orthogonal pilots utilized in the system. Also, the optimal way of assigning the pilots to different users are specified in a closed-form solution. The optimality criterion was to maximize the net sum-rate, which is the sum rate counting only the data transmission portion of the coherence time. It turns out that for many practically meaningful channel scenarios, departing from conventional full pilot reuse and selecting optimal pilot assignment increases the net sum-rate considerably.

This paper expands the concept of optimal pilot assignment to the practical scenario where different user groups exist with different priorities and where it is necessary to maximize the net weighted-sum-rate (WSR). A practical communication system which guarantees sufficient data rates for high-paying selected customers can be considered. We formulate a WSR maximization problem by prioritizing the users into several groups and giving different weights to different groups. The higher priority group would get a higher weight, so that the achievable rate of the higher priority group has a bigger effect on the objective function. We grouped the users by their data rate requirements; in the Internet-of-Things (IoT) era where many different types of devices participate in the network, this kind of differentiation might be helpful. For example, small sensors with less throughput requirement can be considered as lower-priority users, whereas devices with large amount of computation/communication can be considered as higher-priority users. In this paper, we consider two priority groups: preferred user group (1^{st} priority group) and regular user group (2^{nd} priority group), but similar result are expected in general multiple priority groups case, as suggested in Section VII. A closed-form solution for optimal assignment is obtained, which is consistent with intuition. Compared to

the result of [20], the net-WSR of the optimal assignment beats conventional assignment for a wider range of channel coherence time, which means that departing from full pilot reuse and applying optimal less aggressive pilot reuse is necessary particularly in practical net-WSR maximizing scenarios.

This paper is organized as follows. Section II describes the system model for massive MIMO and the pilot contamination effect. Section III summarizes the pilot assignment strategy for multi-cell massive MIMO of [20], which acts as preliminaries for the main analysis of this paper. Section IV formulates the net-WSR-maximizing pilot assignment problem and the closed-form solution is suggested in Section V. Simulation results are included in Section VI, which support the mathematical results of Section V. Here, comparison is made between the performances of the optimal and conventional assignments. In Section VII, further comments on the scenarios with multiple (three or more) priority groups and finite BS antennas are given. Finally, Section VIII concludes the paper.

II. SYSTEM MODEL

A. Multi-Cellular Massive MIMO System

Consider a communication network with L hexagonal cells, where each cell has K single-antenna users located in a uniform-random manner. Each BS with multiple antennas estimates downlink CSIs by uplink pilot training, assuming channel reciprocity in TDD operation. The channel model used in this paper is assumed to be identical to that in [18]; this model fits well with the real-world simulation tested by [21], for both few and many BS antennas. Two types of channel models, independent channel and spatially correlated channel, are used in massive MIMO as stated in [6], while this paper assumes an independent channel model. Antenna elements are assumed to be uncorrelated in this model, which is reasonable with sufficient antenna spacing. The complex propagation coefficient g of a link is decomposed into a complex fast-fading factor h and a slow-fading factor β . The channel link between the m^{th} BS antenna of j^{th} cell and the k^{th} user in the l^{th} cell is modeled as $g_{mjkl} = h_{mjkl}\sqrt{\beta_{jkl}}$. Here, the fast-fading factor h_{mjkl} of each link is modeled as an independent and identically distributed (i.i.d.) complex Gaussian random variable with zero-mean and unit variance. The slow-fading factor β is modeled as $\beta_{jkl} = 1/r_{jkl}^\gamma$ where γ is the signal decay exponent ranging from 2 to 4, and r_{jkl} is the distance between the k^{th} user of the l^{th} cell and the BS of j^{th} cell.

The channel coherence time and channel coherence bandwidth are denoted as T_{coh} and B_{coh} , respectively, while $T_{del} = 1/B_{coh}$ represents the channel delay spread. Here, we define a dimensionless quantity, *normalized coherence time* $N_{coh} = T_{coh}/T_{del} = T_{coh}B_{coh}$, to represent the number of independently usable time-slots available within the coherence time. For a specific numerical example, consider the practical scenario based on OFDM with a frequency smoothness interval of $N_{smooth} = 14$ (i.e., the fast fading coefficient is constant for 14 successive sub-carriers), and a coherence time ranging 20 OFDM symbols. This example has the corresponding normalized coherence time of $N_{coh} = 280$. The normalized coherence time is divided into two parts: pilot training and data

transmission. Based on the CSI estimated in the pilot training phase, data is transmitted in the rest of the coherence time.

B. Pilot Contamination Effect

In a massive MIMO system with TDD operation, K users in each cell are usually assumed to use orthogonal pilots, so that BS can estimate the channel to each user by collecting uplink pilot signals without interference. However, in the multi-cell system, due to a finite N_{coh} value, it is hard to guarantee orthogonality of pilot sets among adjacent cells. Therefore, users in different cells might have non-orthogonal pilot signals, which contaminates the channel estimates of the users. This effect is called the pilot contamination effect, which saturates the achievable rate even as M , the number of BS antennas, increases without bound. The saturation value can be expressed as follows. Assume each cell has a single user, where the identical pilot signal is reused among different cells. Then, the uplink achievable rate of the user in the j^{th} cell is saturated to

$$\lim_{M \rightarrow \infty} R_j = \log_2 \left(1 + \frac{\beta_{jj}^2}{\sum_{l \neq j} \beta_{jl}^2} \right) \quad (1)$$

where β_{jl} represents the slow-fading term of the channel between j^{th} BS and the pilot-sharing user in the l^{th} cell.

III. PRELIMINARIES

In this section, some preliminaries for pilot assignment strategy for multi-cell massive MIMO systems are given. Specifically, our previous work asserts that in some practical circumstances, optimized pilot assignment in a multi-cell massive MIMO system gives much improved sum rate performance than conventional full pilot reuse [20].

A. Hexagonal-Lattice-Based Cell Clustering

First, the locations of different users are assumed to be independent within a cell, and K users in a given cell have orthogonal pilots. Thus the pilot assignment on L cells with K users each can be decomposed into K independent sub-assignments on L cells with single user each.

For identifying which cells reuse the same pilot set, consider an example of hexagonal cells with lattice structure in Fig. 1a. The 3-way partitioning groups the 19 cells into three equidistance subsets colored by red, green and blue. Since each subset in Fig. 1a forms a lattice, we can consider applying this 3-way partitioning in a hierarchical manner as illustrated in Fig. 1b. In the tree structure, the root node represents L cells with three children nodes produced by 3-way partitioning. After i consecutive partitioning, depth i can contain 3^i leaves where each leaf represents $L \cdot 3^{-i}$ cells sharing the same pilot set. With these hierarchical partitioning and tree-like representation, pilot assignment on a multi-cell network can be uniquely represented. The maximally achievable depth of the tree is set to $(\log_3 L - 1)$. This is because the number of pilot-sharing cells need to be greater than 1, since the user who monopolizes a pilot has an infinite achievable rate (from (1)), a meaningless situation. For meaningful analysis, we considered L values with $(\log_3 L - 1) \geq 1$, i.e., $L \geq 9$.

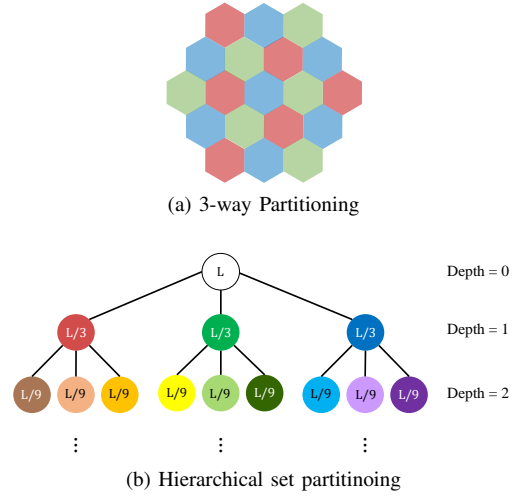


Fig. 1: The Cell Partitioning Method

Another importance associated with identifying the depth of a leaf is that the achievable rate of users in the set of cells corresponding to the leaf depends only on the depth. Let C_i be the achievable rate of a user in a cell at depth i . C_i is an increasing function of i with a nearly linear behavior ($C_{i+1} - C_i \simeq 6$) [20].

B. Pilot Assignment Vector and Net Sum Rate

The tree-like hierarchical representation of pilot assignment strategy can be uniquely converted into a vector form. Let $\mathbf{p} = (p_0, p_1, \dots, p_{\log_3 L - 1})$ be a vector where p_i is the number of leaves in the corresponding tree-like hierarchical representation.

Definition: Let L, K be positive integers. For the given L cells with K users each, the set $P_{L,K}$ of valid pilot assignment vectors for LK users based on 3-way partitioning is given by

$$P_{L,K} = \{ \mathbf{p} = (p_0, p_1, \dots, p_{\log_3 L - 1}) : p_i \in \{0, 1, \dots, K3^i\}, \text{ and } \sum_{i=0}^{\log_3 L - 1} p_i 3^{-i} = K \}$$

For a pilot assignment vector $\mathbf{p} = (p_0, p_1, \dots, p_{\log_3 L - 1})$, the pilot length is defined as $N_{pil}(\mathbf{p}) = \sum_{i=0}^{\log_3 L - 1} p_i$, which represents the number of pilots utilized in the system. Because each element p_i represents the number of leaves at depth i , a total of $L3^{-i}p_i$ users are located at depth i . Recalling C_i is the achievable rate of a user in the i^{th} depth, the per-cell sum rate of the L -cell network with the pilot assignment scheme \mathbf{p} is

$$C_{sum}(\mathbf{p}) = \frac{1}{L} \sum_{i=0}^{\log_3 L - 1} L3^{-i}p_i C_i = \sum_{i=0}^{\log_3 L - 1} 3^{-i}p_i C_i. \quad (2)$$

Considering the actual duration of data transmission after pilot-based channel estimation, the per-cell net sum-rate for a given normalized coherence time N_{coh} can be expressed as

$$C_{net}(\mathbf{p}, N_{coh}) = \frac{N_{coh} - N_{pil}(\mathbf{p})}{N_{coh}} C_{sum}(\mathbf{p}).$$

C. Optimal Pilot Assignment for Multi-User Multi-Cell System

There are two main findings in our previous work [20].

First Finding: With fixed pilot length N_{p0} or, equivalently, fixed time duration allocated to pilot-based channel estimation, the closed form solution for the optimal pilot assignment vector maximizing the per-cell sum rate is found. The optimal solution is formulated as

$$\mathbf{p}'_{opt,K}(N_{p0}) = \arg \max_{\mathbf{p} \in \Omega(N_{p0}, K)} C_{sum}(\mathbf{p}), \quad (3)$$

where $\Omega(N_{p0}, K) = \{\mathbf{p} \in P_{L,K} : N_{pil}(\mathbf{p}) = N_{p0}\}$ is the set of all valid pilot assignment vectors \mathbf{p} , with length of $N_{pil}(\mathbf{p}) = N_{p0}$. The solution is given by $\mathbf{p}'_{opt,K}(N_{p0}) = (p'_0, \dots, p'_{\log_3 L-1})$ where

$$p'_i = \begin{cases} \sum_{t=0}^i K3^t - \frac{N_{p0} - K}{2} & i = \chi(N_{p0}, K) \\ 3 \left(\frac{N_{p0} - K}{2} - \sum_{t=0}^{i-2} K3^t \right) & i = \chi(N_{p0}, K) + 1 \\ 0 & \text{otherwise} \end{cases} \quad (4)$$

with $\chi(N_{p0}, K) = \min\{k : \sum_{i=0}^k K3^i > \frac{N_{p0}-K}{2}\}$ being the first non-zero position of $\mathbf{p}'_{opt,K}(N_{p0})$, i.e., the depth of the least deep leaf node.

Second Finding: The remaining question is that for a given channel coherence time, how much time duration should be allocated to pilot-based channel estimation. Equivalently, with a given N_{coh} , what is the optimal duration N_{p0} for the pilot transmission which maximizes the per-cell net sum-rate. This is given in [20]. For some practical scenarios, the optimal solution has been shown to be far different from the conventional full pilot reuse. Considerable net sum-rate gains were observed in the simulation results.

IV. PILOT ASSIGNMENT STRATEGY FOR NET-WSR MAXIMIZATION

In this section, we provide analysis on pilot assignment strategy for net-WSR maximization. The scenario of using orthogonal pilot sequences possibly larger than K is considered, while users within the same cell are guaranteed to have orthogonal pilots. For ease of analysis, users in different priority groups are assumed to use orthogonal pilots to each other.

A. User Prioritizing

We assume K users in each cell are divided into 2 groups depending on the priority (Section VII deals with the general case where the number of priority groups is greater than 2). Let α be the ratio of the number of 1^{st} priority users to the total number of users ($0 < \alpha < 1$). Let K_1 be the number of 1^{st} priority users in each cell, i.e., $K_1 = \alpha K$. Similarly, K_2 is the number of 2^{nd} priority users in each cell, i.e., $K_2 = (1-\alpha)K$. Considering the scenario with different weights on different user groups, let ω be the weight on the 1^{st} priority group ($0.5 \leq \omega < 1$).

B. Pilot Assignment Vector

For mathematical analysis on pilot assignment strategy, we utilize tools established in [20]: 3-way partitioning and pilot assignment vector representation. First, since we assume users in different priority groups have orthogonal pilots, pilot assignment for the system can be divided into 2 independent sub-assignments: pilot assignment for 1^{st} priority group and then for 2^{nd} priority group. Various available pilot assignments for each group can be easily expressed in a vector form by using the definition in Section III. P_{L,K_1} represents the set of valid pilot assignments for 1^{st} priority group while P_{L,K_2} is used for 2^{nd} priority group.

The set of valid pilot assignments for the entire network (LK users composed of LK_1 users in 1^{st} priority and LK_2 users in 2^{nd} priority) needs to be defined. The set of valid pilot assignments for L cells where each cell has K_1 users in 1^{st} priority group and K_2 users in 2^{nd} priority group can be defined as

$$\tilde{P}_{L,K,\alpha} = \{[\mathbf{p}_1, \mathbf{p}_2] : \mathbf{p}_1 \in P_{L,K_1}, \mathbf{p}_2 \in P_{L,K_2}\}.$$

Therefore, in order to consider all possible pilot assignments $\mathbf{p} \in \tilde{P}_{L,K,\alpha}$ for our system, we need to check possible pairs of $[\mathbf{p}_1, \mathbf{p}_2]$ where \mathbf{p}_1 is a valid assignment for 1^{st} priority users and \mathbf{p}_2 is a valid assignment for 2^{nd} priority users.

C. Problem Formulation

For $\mathbf{p}_1 \in P_{L,K_1}$ and $\mathbf{p}_2 \in P_{L,K_2}$, the corresponding per-cell WSR value is expressed as

$$C_{wsr}(\mathbf{p}_1, \mathbf{p}_2) = \omega C_{sum}(\mathbf{p}_1) + (1 - \omega) C_{sum}(\mathbf{p}_2). \quad (5)$$

Considering the fact that data transmission is available for the portion of coherence time not allocated to pilot training, the per-cell net-WSR is written as

$$C_{net,wsr}(\mathbf{p}_1, \mathbf{p}_2, N_{coh}) = \frac{N_{coh} - [N_{pil}(\mathbf{p}_1) + N_{pil}(\mathbf{p}_2)]}{N_{coh}} C_{wsr}(\mathbf{p}_1, \mathbf{p}_2).$$

Now, we formulate our optimization problem. Let L, K, α , and ω be fixed. For a given N_{coh} value, we want to find out optimal $\mathbf{p}_1 \in P_{L,K_1}$ and $\mathbf{p}_2 \in P_{L,K_2}$ which maximize $C_{net,wsr}(\mathbf{p}_1, \mathbf{p}_2, N_{coh})$. In other words, the optimal pilot assignment vector $\mathbf{p}_{opt}(N_{coh})$ which maximizes net-WSR is

$$\mathbf{p}_{opt}(N_{coh}) = [\mathbf{p}_{opt}^{(1)}(N_{coh}), \mathbf{p}_{opt}^{(2)}(N_{coh})] \\ \triangleq \arg \max_{[\mathbf{p}_1, \mathbf{p}_2] \in \tilde{P}_{L,K,\alpha}} C_{net,wsr}(\mathbf{p}_1, \mathbf{p}_2, N_{coh}).$$

For a given N_{coh} , the \mathbf{p}_{opt} function outputs the optimal pilot assignment pair $[\mathbf{p}_1, \mathbf{p}_2] \in \tilde{P}_{L,K,\alpha}$, where $\mathbf{p}_{opt}^{(i)}(N_{coh})$ is the optimal assignment for the i^{th} priority group.

V. CLOSED-FORM SOLUTION FOR OPTIMAL PILOT ASSIGNMENT

In this section, the closed-form solution to the net-WSR maximization problem is presented. The solution can be obtained in two steps, which are dealt with in the following two subsections, respectively. Subsection A establishes the optimal

pilot assignment rule which maximizes the WSR when the total available number of pilots is given. Subsection B finds the optimal total pilot length which maximizes the net-WSR for a given N_{coh} . Combining these two solutions, we obtain $\mathbf{P}_{opt}(N_{coh})$.

A. Optimal Pilot Assignment Vector under a Total Pilot Length Constraint

Under a constraint on the total pilot length $N_{pil}(\mathbf{p}_1) + N_{pil}(\mathbf{p}_2) = T$, let us find the pilot assignment vector which maximizes $C_{wsr}(\mathbf{p}_1, \mathbf{p}_2)$. This sub-problem can be formulated as

$$\tilde{P}_{opt}(T) = \left\{ [\mathbf{p}_1, \mathbf{p}_2] \in \Theta(T) : \right. \\ \left. C_{wsr}(\mathbf{p}_1, \mathbf{p}_2) \geq C_{wsr}(\mathbf{p}'_1, \mathbf{p}'_2) \quad \forall [\mathbf{p}'_1, \mathbf{p}'_2] \in \Theta(T) \right\}$$

where

$\Theta(T) = \{[\mathbf{p}_1, \mathbf{p}_2] \in \tilde{P}_{L,K,\alpha} : N_{pil}(\mathbf{p}_1) + N_{pil}(\mathbf{p}_2) = T\}$. This optimization problem might have multiple solutions. We thus define the set $\tilde{P}_{opt}(T)$ of optimal pilot assigning strategies. Lemmas 1 and 2 given below specify $\tilde{P}_{opt}(T)$, the set of optimal pilot assignment vectors under the pilot length constraint. Before stating our main Lemmas, we introduce some short-hand notations:

$$\begin{aligned} \mathbb{Z} &= \{\dots, -2, -1, 0, 1, 2, \dots\}, \\ B(T) &= \max(K_1, T - LK_2/3), \\ F(T) &= \min(T - K_2, LK_1/3), \\ S_0(T) &= \{B(T), B(T) + 2, \dots, F(T)\}, \\ S_1(T) &= S_0(T) \setminus \{F(T)\}, \\ g_T(t) &= 3^{\chi(t, K_1) - \chi(T-t-2, K_2)} \frac{1-\omega}{\omega}. \end{aligned}$$

where $\chi(N_{p0}, K) = \min\{k : \sum_{i=0}^k K3^i > \frac{N_{p0}-K}{2}\}$ as defined in section III-C.

The total pilot length $N_{pil}(\mathbf{p}_1) + N_{pil}(\mathbf{p}_2) = T$ can be decomposed into two parts: pilot length $N_{pil}(\mathbf{p}_1) = t$ for 1st priority group and pilot length $N_{pil}(\mathbf{p}_2) = T - t$ for 2nd priority group. From [20], $N_{pil}(\mathbf{p}_1) \in \{K_1, K_1 + 2, \dots, LK_1/3\}$ and $N_{pil}(\mathbf{p}_2) \in \{K_2, K_2 + 2, \dots, LK_2/3\}$ holds for $[\mathbf{p}_1, \mathbf{p}_2] \in \tilde{P}_{L,K,\alpha}$, so that we can obtain the set of possible $[N_{pil}(\mathbf{p}_1), N_{pil}(\mathbf{p}_2)]$ pairs illustrated in Table I. As seen in the Table, $B(T)$ represents the minimum possible value assigned for 1st priority group, and $F(T)$ is the maximum possible value assigned for 1st priority group (Note that $B(T) \leq F(T)$ by definition). $S_0(T)$ represents the set of possible values assigned for 1st priority group. Later, it can be seen that $g_T : S_1(T) \rightarrow \mathbb{R}$ is defined for comparing C_{wsr} values of different assignments. Now we state our main Lemmas.

Lemma 1. *If $\log_3 \frac{\omega}{1-\omega} \notin \mathbb{Z}$, then the set $\tilde{P}_{opt}(T)$ of optimal pilot assignment vectors maximizing C_{wsr} is*

$$\tilde{P}_{opt}(T) = \left\{ [\mathbf{p}'_{opt, K_1}(\rho(T)), \mathbf{p}'_{opt, K_2}(T - \rho(T))] \right\} \quad (6)$$

TABLE I: Possible pilot length pairs for each priority group

$N_{pil}(\mathbf{p}_1) = t$	$N_{pil}(\mathbf{p}_2) = T - t$
$B(T)$	$T - B(T)$
$B(T) + 2$	$T - B(T) - 2$
\vdots	\vdots
$F(T) - 2$	$T - F(T) + 2$
$F(T)$	$T - F(T)$

where

$$\rho(T) = \begin{cases} B(T), & \text{if } S_1(T) = \emptyset \text{ or } g_T(B(T)) > 1 \\ F(T), & \text{else if } g_T(F(T) - 2) < 1 \\ \min\{t \in S_1(T) : g_T(t) \geq 1\}, & \text{otherwise.} \end{cases} \quad (7)$$

As stated in Lemma 1, there exists unique optimal vector $[\mathbf{p}'_{opt, K_1}(\rho(T)), \mathbf{p}'_{opt, K_2}(T - \rho(T))]$ for every ω satisfying $\log_3 \frac{\omega}{1-\omega} \notin \mathbb{Z}$. However, in the case of $\log_3 \frac{\omega}{1-\omega} \in \mathbb{Z}$, we have possibly multiple optimal solutions as specified in the following Lemma.

Lemma 2. *If $\log_3 \frac{\omega}{1-\omega} \in \mathbb{Z}$, then the set $\tilde{P}_{opt}(T)$ of optimal pilot assignment vectors maximizing C_{wsr} is*

$$\tilde{P}_{opt}(T) = \left\{ [\mathbf{p}'_{opt, K_1}(t), \mathbf{p}'_{opt, K_2}(T - t)] : \right. \\ \left. t \in \{\rho(T), \rho(T) + 2, \dots, \mu(T)\} \right\} \quad (8)$$

where $\rho(T)$ is as defined in (7) and

$$\mu(T) = \begin{cases} B(T), & \text{if } S_1(T) = \emptyset \text{ or } g_T(B(T)) > 1 \\ F(T), & \text{else if } g_T(F(T) - 2) < 1 \\ \min\{t \in S_1(T) : g_T(t) \leq 1\} + 2, & \text{otherwise.} \end{cases}$$

We defer the proofs of Lemmas 1 and 2 to Appendix A. These two lemmas lead to our first main theorem, which specifies an element of $\tilde{P}_{opt}(T)$ as a function of T .

Theorem 1. *For given total pilot length $T \in \{K, K + 2, \dots, LK/3\}$, using pilot assignment vector $\mathbf{p}'_{opt, K_1}(\rho(T))$ for 1st priority group and $\mathbf{p}'_{opt, K_2}(T - \rho(T))$ for 2nd priority group maximizes the WSR. This optimal solution allocates $\rho(T)$ pilots to 1st priority group and $T - \rho(T)$ to 2nd priority group. In other words,*

$$[\mathbf{p}'_{opt, K_1}(\rho(T)), \mathbf{p}'_{opt, K_2}(T - \rho(T))] \in \tilde{P}_{opt}(T). \quad (9)$$

Proof From (6) and (8), we can confirm that (9) holds, irrespective of ω value. \square

When $\log_3 \frac{\omega}{1-\omega} \notin \mathbb{Z}$ holds, $\tilde{P}_{opt}(T)$ contains unique element as stated in (6) or (9). In the case of $\log_3 \frac{\omega}{1-\omega} \in \mathbb{Z}$, $\tilde{P}_{opt}(T)$ might have multiple elements as in (8), but we can guarantee the existence of an element stated in (9). Here, we attempt to get some insight on $\rho(T)$ in (7), the optimal pilot length for 1st priority group. The following proposition suggests an alternative expression for $\rho(T)$, depending on the range of T .

Proposition 1. Let $s = \lceil \log_3 \frac{w}{1-w} \rceil$. If $3^s \geq L/3$,

$$\rho(T) = \begin{cases} T - K_2 & \text{if } K \leq T \leq K_2 + \frac{LK_1}{3} \\ LK_1/3 & \text{if } K_2 + \frac{LK_1}{3} < T \leq \frac{LK}{3} \end{cases} \quad (10)$$

Otherwise (i.e., $3^s < L/3$),

$$\rho(T) = \begin{cases} T - K_2 & \text{if } K \leq T \leq K_2 + 3^s K_1 \\ \phi(T) & \text{if } K_2 + 3^s K_1 < T < \frac{LK_1}{3} + \frac{LK_2}{3^{s+1}} \\ LK_1/3 & \text{if } \frac{LK_1}{3} + \frac{LK_2}{3^{s+1}} \leq T \leq \frac{LK}{3} \end{cases} \quad (11)$$

where

$$\phi(T) = \begin{cases} 3^{V(T)+s-1} K_1 & \text{if } T \leq 3^{V(T)+s-1} K_1 + 3^{V(T)} K_2 \\ T - 3^{V(T)} K_2 & \text{if } T > 3^{V(T)+s-1} K_1 + 3^{V(T)} K_2, \end{cases}$$

$$V(T) = \min\{i \in \{0, 1, \dots, \log_3 L - 1 - s\} : T \leq 3^{s+i} K_1 + 3^i K_2\}.$$

TABLE II: Optimal pilot lengths for each priority group

(a) $3^s \geq L/3$ case

T	$\rho(T)$	$T - \rho(T)$
K	K_1	K_2
$K + 2$	$K_1 + 2$	
\vdots	\vdots	
$K_2 + \frac{LK_1}{3}$	$\frac{LK_1}{3}$	$K_2 + 2$
$K_2 + \frac{LK_1}{3} + 2$	$\frac{LK_1}{3}$	
\vdots	$\frac{LK_1}{3}$	
$\frac{LK}{3}$	$\frac{LK_2}{3}$	

(b) $3^s < L/3$ case

T	$\rho(T)$	$T - \rho(T)$	d_1	d_2
K	K_1		0	
$K + 2$	$K_1 + 2$		0	
\vdots	\vdots	K_2	\vdots	0
$K_2 + 3^s K_1 - 2$	$3^s K_1 - 2$		$s - 1$	
$K_2 + 3^s K_1$	$3^s K_1$	s		
$K_2 + 3^s K_1 + 2$	$3^s K_1 + 2$	$K_2 + 2$	s	0
\vdots	\vdots	\vdots	\vdots	\vdots
$3K_2 + 3^s K_1 - 2$	$3^s K_1 - 2$	$3K_2 - 2$	s	0
$3K_2 + 3^s K_1$	$3^s K_1$	$3K_2$	s	1
$3K_2 + 3^s K_1 + 2$	$3^s K_1 + 2$	\vdots	\vdots	\vdots
\vdots	\vdots	$3K_2$	\vdots	1
$3K_2 + 3^{s+1} K_1$	$3^{s+1} K_1$	\vdots	$s + 1$	\vdots
\vdots	\vdots	\vdots	\vdots	\vdots
$\frac{LK_1}{3} + \frac{LK_2}{3^{s+1}}$	$\frac{LK_1}{3}$	$\frac{LK_2}{3^{s+1}}$		
\vdots	\vdots	\vdots		
$\frac{LK}{3}$	$\frac{LK_2}{3}$	$\frac{LK_2}{3}$		

The detailed proof for Proposition 1 is in Appendix B, but here we provide a brief explanation on the result that is consistent with our intuition. As T increases, variation of $\rho(T)$ has a pattern illustrated in Tables IIa. When ω is sufficiently large ($3^s \geq L/3$ case, Table IIa), the WSR is mostly determined by the sum rate of the 1st priority group. Therefore, the WSR-maximizing solution first allocates additional pilot

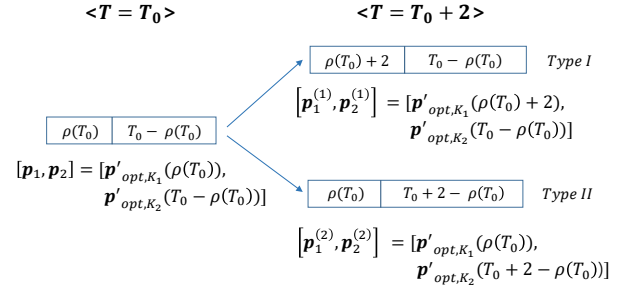


Fig. 2: Analysis on Proposition 1

resources to the 1st priority group up to its maximum pilot length $LK_1/3$. After the 1st group gets maximum available pilot resources, additional pilot is dedicated to the 2nd priority group. In the case of $3^s < L/3$ (Table IIb), weight ω on the 1st priority group is not large enough so that the optimal pilot resource allocation rule has an alternative pattern for two priority groups, as illustrated below.

Consider the optimal assignment for $T = T_0$, as shown in left side of Fig. 2. When additional pilot resource is available, we can consider two types of assignments for $T = T_0 + 2$: Type I allocates extra pilots to 1st priority group, while Type II allocates extra pilots to 2nd priority group. From Corollary 1 of [20], $\mathbf{p}_1^{(1)}$ can be obtained by tossing 1 from the left-most non-zero element of \mathbf{p}_1 to increase the adjacent element by 3 (Similar relationship exists for $\mathbf{p}_2^{(2)}$ and \mathbf{p}_2). Denote the left-most non-zero element of \mathbf{p}_1 and \mathbf{p}_2 by $d_1 = \chi(\rho(T_0), K_1)$ and $d_2 = \chi(T - \rho(T), K_2)$, respectively. Then from the WSR expression (5), Type I allocation increases the WSR by $\omega L 3^{-d_1} (C_{d_1+1} - C_{d_1})$ and Type II allocation yields an increase by $(1 - \omega) L 3^{-d_2} (C_{d_2+1} - C_{d_2})$, compared to the WSR of $[\mathbf{p}_1, \mathbf{p}_2]$ allocation.

Therefore, when the total pilot length is $T_0 + 2$, the optimal solution is chosen by comparing $\omega L 3^{-d_1} (C_{d_1+1} - C_{d_1})$ and $(1 - \omega) L 3^{-d_2} (C_{d_2+1} - C_{d_2})$. Using $C_{i+1} - C_i \simeq \text{const.}$, this reduces to comparing s and $d_1 - d_2$. In summary, as T increases by 2, additional 2 pilots are assigned to either 1st or 2nd priority group, where the decision is based on the sign of $s - (d_1 - d_2)$. For example, consider $T = 3K_2 + 3^s K_1$ in Table IIb. Since $d_1 = s$ and $d_2 = 1$, we have $s > d_1 - d_2$. Therefore, assigning the additional pilot to 1st priority group is the WSR-maximizing choice, so that $\rho(T + 2) = \rho(T) + 2 = 3^s K_1 + 2$ as in the Table. Note that d_1 increases as $\rho(T)$ increases, while d_2 increases as $T - \rho(T)$ increases. Therefore, considering the sign of $s - (d_1 - d_2)$, balanced resource allocation occurs as additional pilot resource is allowed. This alternative allocation occurs until $T < \frac{LK_1}{3} + \frac{LK_2}{3^{s+1}}$.

When $T = \frac{LK_1}{3} + \frac{LK_2}{3^{s+1}}$, the optimal number of pilots for the 1st priority group reaches $\frac{LK_1}{3}$, the maximum possible value. Therefore, similar to the $3^s \geq L/3$ case, for T values greater than the threshold value, the additional pilot is dedicated to the 2nd priority group. From this observation, we can directly obtain the following proposition, which relates the consecutive $\rho(T)$ values as T increases. The proof of the proposition is in Appendix B.

Proposition 2. Either $\rho(T+2) = \rho(T)$ or $\rho(T+2) = \rho(T) + 2$

holds for $T \in \{K, K+2, \dots, \frac{LK}{3} - 2\}$.

B. Optimal Total Pilot Length for Given Channel Coherence Time

In this subsection, we solve the second sub-problem: for a given normalized coherence time N_{coh} , find the optimal total pilot length T which maximizes the net-WSR. Here, we define the maximum WSR value under the constraint on the total pilot length T as

$$\bar{C}_{wsr}(T) = \max_{\{\mathbf{p}_1, \mathbf{p}_2\} \in \Theta(T)} C_{wsr}(\mathbf{p}_1, \mathbf{p}_2).$$

By using (9), we can relate $\bar{C}_{wsr}(T)$ and $\bar{C}_{wsr}(T+2)$ as in the following Corollary, proof of which is given in Appendix C.

Corollary 1. For $T \in \{K, K+2, \dots, \frac{LK}{3} - 2\}$,

$$\bar{C}_{wsr}(T+2) = \bar{C}_{wsr}(T) + \delta_T$$

holds where

$$\delta_T = \begin{cases} \delta_T^{(2)} & T \geq \frac{LK_1}{3} + \max\{\frac{L}{3^{s+1}}, 1\} K_2 \\ \max\{\delta_T^{(1)}, \delta_T^{(2)}\} & \text{otherwise,} \end{cases}$$

$$\delta_T^{(1)} = \omega L 3^{-d_1} (C_{d_1+1} - C_{d_1}),$$

$$\delta_T^{(2)} = (1 - \omega) L 3^{-d_2} (C_{d_2+1} - C_{d_2}),$$

$$d_1 = \chi(\rho(T), K_1), \text{ and } d_2 = \chi(T - \rho(T), K_2).$$

Note that $\{C_i\}$ is defined in Section III-A. Corollary 1 implies that $\bar{C}_{wsr}(T)$ is an increasing function of T . Now, using Corollary 1, we proceed to find the solution for the optimal total pilot length for a given N_{coh} , as stated in Theorem 2 below. Define

$$\begin{aligned} h_T(N_{coh}) &\triangleq C_{net,wsr}(\mathbf{p}'_{opt,K_1}(\rho(T)), \mathbf{p}'_{opt,K_2}(T - \rho(T)), N_{coh}) \\ &= \frac{N_{coh} - T}{N_{coh}} \bar{C}_{wsr}(T), \end{aligned}$$

which is the maximum net-WSR value for a given pilot length T . Note that $h_T(N_{coh})$ is an increasing function of N_{coh} , which is positive for $N_{coh} > T$ and saturates to $\bar{C}_{wsr}(T)$ as N_{coh} goes to infinity. Consider a plot of this function for $T = K, K+2, \dots, LK/3$. Using the fact that $\bar{C}_{wsr}(T)$ is an increasing function of T , we can check that the curve $h_T(N_{coh})$ is above other curves for $K\Delta_{\frac{T-K}{2}} \leq N_{coh} < K\Delta_{\frac{T-K}{2}+1}$ where

$$\Delta_n = \begin{cases} 0, & n = 0 \\ \left\{ 2n + K + \frac{2\bar{C}_{wsr}(2n+K+2)}{\delta_{2n+K}} \right\} / K, & 1 \leq n \leq N_L \\ \infty, & n = N_L + 1. \end{cases}$$

and $N_L = \frac{LK/3-K}{2}$ (detailed analysis is in Appendix D). Therefore, $K\Delta_n$ represents consecutive N_{coh} values where optimal assignment changes. Using this definition, we now state our second main theorem, specifying $\mathbf{p}_{opt}(N_{coh})$. The proof of the theorem is in Appendix D.

Theorem 2. If the given normalized coherence time N_{coh} satisfies $\Delta_n \leq N_{coh}/K < \Delta_{n+1}$, the optimal pilot assignment

$\mathbf{p}_{opt}(N_{coh}) = [\mathbf{p}_{opt}^{(1)}(N_{coh}), \mathbf{p}_{opt}^{(2)}(N_{coh})]$ that maximizes net-WSR $C_{net,wsr}$ has the following form:

$$\begin{aligned} \mathbf{p}_{opt}^{(1)}(N_{coh}) &= \mathbf{p}'_{opt,K_1}(\rho(2n+K)) \\ \mathbf{p}_{opt}^{(2)}(N_{coh}) &= \mathbf{p}'_{opt,K_2}(2n+K - \rho(2n+K)). \end{aligned} \quad (12)$$

Also, the optimal number of pilots is

$$N_{pil}(\mathbf{p}_{opt}^{(1)}(N_{coh})) + N_{pil}(\mathbf{p}_{opt}^{(2)}(N_{coh})) = 2n + K.$$

For any positive N_{coh} value, there exists an integer $0 \leq n \leq N_L$ such that $N_{coh} \in [K\Delta_n, K\Delta_{n+1})$. The optimal assignment for a given N_{coh} is specified by the corresponding n values, as in (12). In other words, the optimal pilot assignment for the 1st priority group turns out to be $\mathbf{p}'_{opt,K_1}(\rho(2n+K))$, while for the 2nd priority group we have $\mathbf{p}'_{opt,K_2}(2n+K - \rho(2n+K))$. Combining with (4), we can obtain the exact components of the optimal pilot vector. Also, we can figure that the optimal number of pilots utilized in the system is $N_{pil}(\mathbf{p}_{opt}^{(1)}(N_{coh})) + N_{pil}(\mathbf{p}_{opt}^{(2)}(N_{coh})) = 2n + K$ for N_{coh} values satisfying $\Delta_n \leq N_{coh}/K < \Delta_{n+1}$.

VI. SIMULATION RESULTS

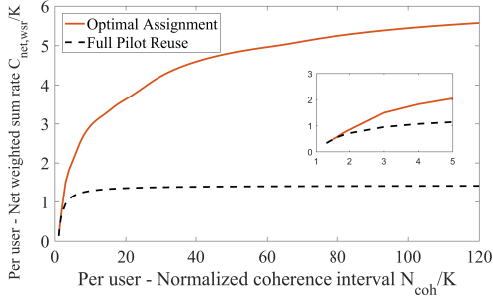
In this section, the effect of utilizing optimal assignment is analyzed, based on simulation results. The optimal solution depends on C_i values in (2), which need to be obtained by simulation. C_i depends on β terms in (1), which is a function of distance between interfering users. Since the location of each user within a cell is assumed to be uniform-random, the β terms need to be generated in pseudo-random manner by simulation. Following the settings in [18], the signal decay exponent is $\gamma = 3.7$, the cell radius is r meters, and the cell-hole radius is $0.14r$. Note that $\{C_i\}$ values do not depend on r . The computation of C_i values proceeds by taking average of 100,000 pseudo-random trials on user location. The system with $L = 81$ cells and $K = 10$ users in each cell was considered.

Based on the simulation result of C_i , WSR values for various possible pilot assignments can be computed. From the WSR data, the optimal pilot assignment which maximizes net-WSR $C_{net,wsr}$ for a given N_{coh} can be obtained, as listed in Table III. $K = 10$ and $\alpha = 0.2$ imply that each cell has 2 users with 1st priority and 8 users with 2nd priority. We can check that the list of Table III is consistent with the mathematical result in Theorem 2. For example, when $19 \leq N_{coh} < 23$ (or $\Delta_1 = 1.9 \leq N_{coh}/K < 2.3 = \Delta_2$), according to (12) with $n = 1$, we have $\mathbf{p}_{opt}^{(1)}(N_{coh}) = \mathbf{p}'_{opt,K_1}(\rho(K+2)) = \mathbf{p}'_{opt,K_1}(4) = (1, 3, 0, 0)$, where the last two equalities are from (7) and (4), respectively. Similarly, we obtain $\mathbf{p}_{opt}^{(2)}(N_{coh}) = (8, 0, 0, 0)$ which coincide with the result of Table III. In practice, utilizing $N_{pil}(\mathbf{p}_1) + N_{pil}(\mathbf{p}_2) = 12$ pilots by applying pilot assignment $(1, 3, 0, 0)$ for 1st priority group and $(8, 0, 0, 0)$ for 2nd priority group maximizes the net-WSR of the system, when the given N_{coh} satisfies $\Delta_1 = 1.9 \leq N_{coh}/K < 2.3 = \Delta_2$.

A certain trend in optimal pilot assignment is revealed in Table III. As N_{coh}/K value increases, optimal pilot assignment for one priority group changes while optimal assignment

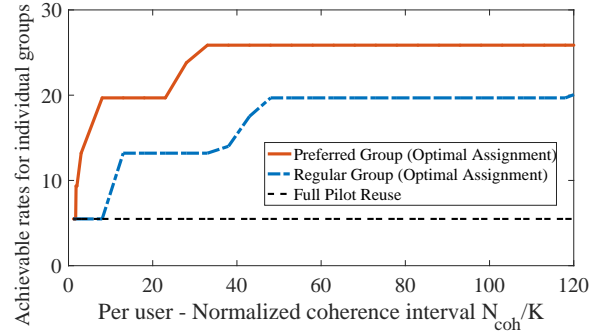
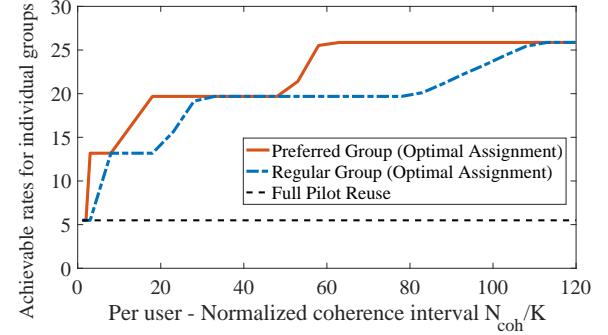
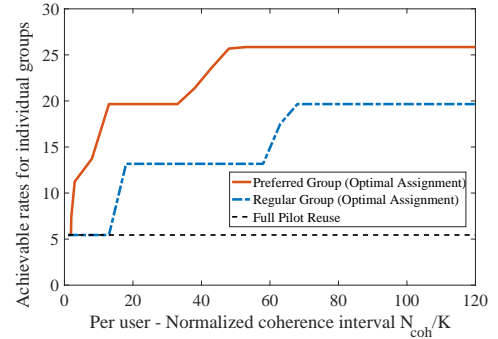
TABLE III: Optimal pilot assignment ($L = 81, K = 10, \alpha = 0.2, \omega = 0.7$)

N_{coh}/K	\mathbf{p}_1 $= \mathbf{p}_{opt}^{(1)}(N_{coh})$	\mathbf{p}_2 $= \mathbf{p}_{opt}^{(2)}(N_{coh})$	$N_{pil}(\mathbf{p}_1)$ $+ N_{pil}(\mathbf{p}_2)$
$0 \sim 1.9$	(2, 0, 0, 0)	(8, 0, 0, 0)	10
$1.9 \sim 2.3$	(1, 3, 0, 0)	(8, 0, 0, 0)	12
$2.3 \sim 4.3$	(0, 6, 0, 0)	(8, 0, 0, 0)	14
$4.3 \sim 4.7$	(0, 6, 0, 0)	(7, 3, 0, 0)	16
$4.7 \sim 5.1$	(0, 6, 0, 0)	(6, 6, 0, 0)	18
\vdots	\vdots	\vdots	\vdots
$122 \sim$	(0, 0, 0, 54)	(0, 0, 0, 216)	270

Fig. 3: Per-user Net-WSR for optimal/conventional pilot assignments ($L = 81, K = 10, \alpha = 0.2, \omega = 0.9$)

for the other priority group remains the same. For example, optimal pilot assignment for 1st priority group changes from (1, 3, 0, 0) to (0, 6, 0, 0) while optimal assignment for 2nd priority group remains as (8, 0, 0, 0), when N_{coh}/K value changes near 2.3. On the other hand, optimal pilot assignment for 1st priority group remains as (0, 6, 0, 0), while optimal assignment for 2nd priority group changes from (7, 3, 0, 0) to (6, 6, 0, 0), when N_{coh}/K value changes near 4.7. This result is consistent with the message of Theorem 2. It is shown that the optimal assignment has the form of (12), with n increasing as N_{coh}/K grows. Combining with Proposition 2, we see that the optimal pilot length of the 1st priority group either increases by 2 or remains the same, as n grows. In other words, as N_{coh}/K increases, we are allowed to use two extra pilots, and which group to allocate the extra pilots is based on α and ω .

Now, we compare the net-WSR values of optimal assignment and conventional assignment. Here, conventional assignment means assigning K orthogonal pilots reused in each cell. Fig. 3 shows net-WSR comparison for $L = 81, K = 10, \alpha = 0.2$, and $\omega = 0.9$. As per user - normalized coherence interval N_{coh}/K increases, optimal assignment has substantial net-WSR gains compared to conventional assignment. In the inset of Fig. 3, we have a plot focusing on low N_{coh}/K values. For N_{coh}/K greater than 1.7, optimal assignment beats the conventional full reuse. In the case of maximizing per-user net-rate C_{net}/K in [20], optimal assignment beats full reuse for N_{coh}/K greater than 6.2. Therefore, departing from conventional wisdom is beneficial for a wider N_{coh}/K range, compared to the scenario where maximizing the net-rate was the objective. A considerable increase of per-user net-WSR is seen even at low N_{coh}/K values. For $N_{coh}/K = 5, 10$ and 20, optimal assignment has 79.8%, 130.2% and 169.0% higher

(a) $\alpha = 0.2, \omega = 0.8$ (b) $\alpha = 0.2, \omega = 0.6$ (c) $\alpha = 0.4, \omega = 0.8$ Fig. 4: Per-user achievable rates of each priority group for optimal/conventional pilot assignments ($L = 81, K = 10$)

net-WSRs than conventional assignment.

Now, we analyze the achievable rate averaged over each priority group. Figs. 4a, 4b and 4c illustrate per-user achievable rates in the case of using conventional assignment versus optimal assignment, with different α and ω settings. In the case of conventional assignment, every user has a constant achievable rate value irrespective of N_{coh}/K , since the assignment rule is fixed so that the effect of pilot contamination does not change. However, in the case of choosing optimal assignment specific to given N_{coh}/K to maximize the net-WSR, each priority group can enjoy a higher achievable rate by utilizing extra pilots and spreading pilot-sharing users, which reduces the pilot contamination effect. The allocation of extra pilots to the preferred group or the regular group depends on system setting: α and ω .

Consider a case where α is fixed to 0.2 and compare achievable rate curves for $\omega = 0.8$ and 0.6 (Figs. 4a and 4b,

TABLE IV: Optimal pilot lengths for each priority group (3 priority group case - $L = 27$, $K = 10$, $\alpha_1 = \omega_3 = 0.2$, $\alpha_2 = \omega_2 = 0.3$, $\alpha_3 = \omega_1 = 0.5$)

T	10	12	14	16	18	20	22	24	...	30	32	34	...	42
$\rho_1(T)$	2	4	6						8		10	...	18	
$\rho_2(T)$	3		5	7	9									
$\rho_3(T)$	5				7		9	...	15					

T	44	46	...	60	62	64	...	90
$\rho_1(T)$	18							
$\rho_2(T)$	11	13	...	27				
$\rho_3(T)$	15		17		19	...	45	

respectively). We can observe that a larger ω value implies a wider performance gap between the preferred group and the regular group. This can be explained as follows. As we have a higher ω value, the influence of preferred group performance to the cost function (net-WSR) increases, so that it is more preferable to use extra pilots for 1st priority group rather than 2nd priority group, in order to maximize the net-WSR (note that the performance gap converges to zero, since the individual rates cannot exceed $C_{\log_3 L-1}$ as mentioned in Section III-A). Now, consider a scenario where ω is fixed to 0.8 and compare the achievable rate curves for $\alpha = 0.2$ and 0.4 (Figs. 4a and 4c, respectively). We can observe that as α increases, we have more users under 1st priority, which requires more resources (coherence time) to boost up the achievable rate of the preferred group. Consequently, the achievable rate of the regular group increases slowly as α increases, as shown in the figures.

VII. FURTHER COMMENTS

A. Comments on Multiple Priority Groups

The scenario of having multiple priority groups (greater than two) is considered in this subsection. Based on the mathematical analysis and simulation result obtained from the two priority group case, the result for the generalized setting can be anticipated. For the general case of n priority groups, denote weight/ratio of i^{th} priority group as ω_i and α_i , respectively. The net-WSR maximization problem can be formulated as finding

$$\begin{aligned} \mathbf{p}_{opt}(N_{coh}) &= [\mathbf{p}_{opt}^{(1)}(N_{coh}), \dots, \mathbf{p}_{opt}^{(n)}(N_{coh})] \\ &\triangleq \arg \max_{[\mathbf{p}_1, \dots, \mathbf{p}_n]} C_{net,wsr}(\mathbf{p}_1, \dots, \mathbf{p}_n, N_{coh}) \end{aligned}$$

where $\mathbf{p}_i \in P_{L, \alpha_i K}$ for $i = 1, \dots, n$. Here,

$$\begin{aligned} C_{net,wsr}(\mathbf{p}_1, \dots, \mathbf{p}_n, N_{coh}) \\ = \frac{N_{coh} - \sum_{i=1}^n N_{pil}(\mathbf{p}_i)}{N_{coh}} C_{wsr}(\mathbf{p}_1, \dots, \mathbf{p}_n) \end{aligned}$$

and $C_{wsr}(\mathbf{p}_1, \dots, \mathbf{p}_n) = \sum_{i=1}^n \omega_i C_{sum}(\mathbf{p}_i)$.

Similar to the two priority group case, the problem can be divided into two sub-problems: 1) solving the optimal pilot assignment rule under the constraint of $\sum_{i=1}^n N_{pil}(\mathbf{p}_i) = T$, and 2) obtaining optimal T value for a given N_{coh} . The solution to the 1st sub-problem determines the optimal pilot length $\rho_1(T), \dots, \rho_n(T)$ for each priority group (In the two-group case, the optimal lengths were $\rho(T)$ and $T - \rho(T)$). For

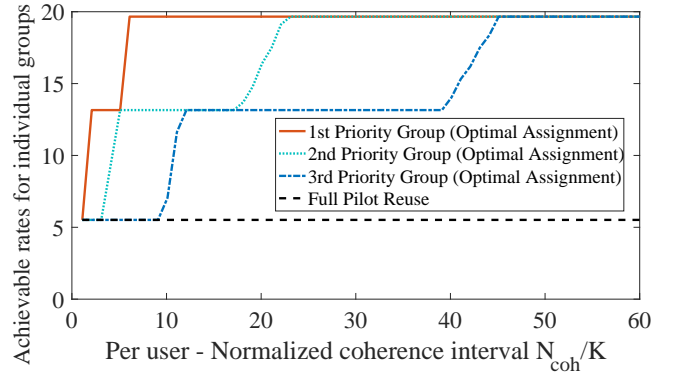


Fig. 5: Per-user achievable rates of each priority group for optimal/conventional pilot assignments ($L = 27$, $K = 10$, $[\alpha_1, \alpha_2, \alpha_3] = [0.1, 0.4, 0.5]$, $[\omega_1, \omega_2, \omega_3] = [0.7, 0.2, 0.1]$)

a simple scenario as an example, the result of pilot resource allocation is expressed in Table IV. The system with $L = 27$ cells and $K = 10$ users per cell is assumed. The weight/ratio for three priority groups is fixed as $\alpha_1 = \omega_3 = 0.2$, $\alpha_2 = \omega_2 = 0.3$, $\alpha_3 = \omega_1 = 0.5$.

Similar to Table IIa and IIb, the optimal pilot allocation to three priority groups has a certain pattern. As T increases (i.e., additional pilots are allowed), one of three priority groups obtains extra pilots alternatively. Considering the WSR increment of allocating extra pilots to each priority group, optimal assignment chooses the priority group which maximizes the increment. Since the increment is proportional to ω_i value, the optimal rule chooses from a higher priority group to a lower priority group, sequentially. Therefore, in the general case of multiple priority groups, the pilot assignment rule for each priority group has certain characteristic which is easily obtained from the mathematical analysis on the two-group case. Under the scenario of three priority groups, Fig. 5 illustrates the achievable rate averaged over each priority group. The system parameters are set to $L = 27$, $K = 10$, $\alpha_1 = 0.1$, $\alpha_2 = 0.4$, $\alpha_3 = 0.5$, $\omega_1 = 0.7$, $\omega_2 = 0.2$, $\omega_3 = 0.1$. Similar to the scenario with two priority groups, each priority group can enjoy a higher achievable rate by applying the net-WSR maximizing pilot assignment.

B. Comments on finite antenna elements case

This paper considers the scenario of having an infinite number of BS antennas in the mathematical analysis. However, a finite number of antennas will be deployed at each BS in practice, so that the performance of the suggested pilot assignment scheme needs to be confirmed for finite antenna elements. By Theorem 1 of [18], the achievable rate of massive MIMO with pilot reuse factor β can be obtained for finite M . Based on this result, the net-WSR maximizing optimal pilot assignment for finite M is numerically obtained. Fig. 6 illustrates the performance of optimal/conventional pilot assignment as a function of M . The receivers with maximal-ratio-combining (MRC) and zero-forcing-combining (ZFC) are compared, and the system parameters are assumed to be $L = 81$, $K = 10$, $\alpha = 0.2$, $\omega = 0.7$ and $N_{coh} = 200$. In both MRC and ZFC receivers, the optimal assignment has

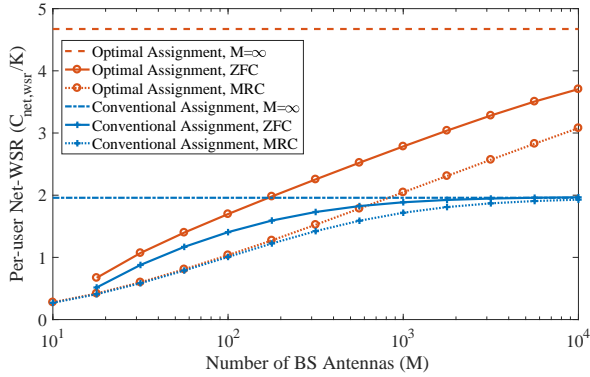


Fig. 6: Per-user Net-WSR versus M for optimal/conventional pilot assignments

a performance gain compared to the conventional full pilot reuse, even in practical scenarios [4], [21] of having 128 antennas at each BS. Under the assumption of using optimal assignment, the receivers with ZFC and MRC has a non-decreasing performance gap. This implies that an appropriate signal processing scheme can boost up the performance gain of optimal pilot assignment.

VIII. CONCLUSION

In a massive MIMO system with users grouped by priority, the optimal way of assigning pilots and the optimal portion of pilot training time to maximize the net-WSR have been found in a closed-form solution. As the available time slot N_{coh} increases, the optimal strategy allows more time on pilot transmission, the allocation of extra pilot training time to either priority group depends on the weight ω and portion α . Compared to the net sum-rate-maximization problem, our closed-form solution has better performance than conventional assignment for a wider range of N_{coh}/K values, which means that our optimal solution can be applied to various practical channel scenarios. Simulation results of individual group achievable rates show that both groups can guarantee higher rates than conventional full pilot reuse, while a performance gap between the preferred/regular groups exists due to the different weights. The generalized scenario with multiple priority groups (greater than two) is also analyzed based on the insights obtained from the two-group case.

APPENDIX A PROOFS OF LEMMA 1, LEMMA 2

Given the total pilot length T , it can be decomposed into two parts: pilot length t for 1st priority group, and pilot length $T-t$ for 2nd priority group (as in the Table I). Note that under the constraint on the pilot length t for 1st group, we already know that $\mathbf{p}'_{opt,K_1}(t)$ maximizes C_{sum} from (3). Similar results hold for 2nd group. Therefore, when t is fixed, we can obtain that $[\mathbf{p}'_{opt,K_1}(t), \mathbf{p}'_{opt,K_2}(T-t)]$ maximizes C_{wsr} . However, a given T can be decomposed into many possible $(t, T-t)$ pairs (note that the possible t values are specified as $S_0(T)$). All we need to find is optimal t , the pilot length for 1st group.

Let $f(t) = C_{wsr}(\mathbf{p}'_{opt,K_1}(t), \mathbf{p}'_{opt,K_2}(T-t))$. Then, using Corollary 1 of [20] and approximating C_i as a linear function ($C_{i+1} - C_i \simeq 6$), we have

$$f(t) - f(t+2) = 6\omega 3^{-\chi(t,K_1)}(g_T(t) - 1). \quad (13)$$

Therefore, WSR comparison for two consecutive candidates $[\mathbf{p}'_{opt}(t, K_1), \mathbf{p}'_{opt}(T-t, K_2)]$ and $[\mathbf{p}'_{opt}(t+2, K_1), \mathbf{p}'_{opt}(T-t-2, K_2)]$ can be simplified by checking the sign of $g_T(t) - 1$ for $t \in S_1(T)$.

A. Proof of Lemma 1

For T values with $S_1(T) = \emptyset$, $S_0(T)$ has a single element $B(T)$, so that $[\mathbf{p}'_{opt,K_1}(B(T)), \mathbf{p}'_{opt,K_2}(T-B(T))]$ is optimal trivially. The following proof deals with T values with $S_1(T) \neq \emptyset$. Note that when $\log_3 \frac{\omega}{1-\omega} \notin \mathbb{Z}$, we have no $t \in S_1(T)$ such that $g_T(t) = 1$. Using (13) and the fact that $g_T(t)$ is monotone increasing in t , we obtain optimal t_0 which maximizes $f(t)$ among $t \in S_0(T)$. The proof is divided into three cases.

First, if $g_T(B(T)) > 1$, we have $g_T(t) > 1$ (i.e., $f(t) > f(t+2)$) $\forall t \in S_1(T)$, so that $B(T)$ maximizes $f(t)$ among $t \in S_0(T)$. Second, if $g_T(F(T)-2) < 1$, we have $g_T(t) < 1$ (i.e., $f(t) < f(t+2)$) $\forall t \in S_1(T)$, so that $F(T)$ maximizes $f(t)$ among $t \in S_0(T)$. Finally, for the else case (i.e., $g_T(B(T)) \leq 1 \leq g_T(F(T)-2)$), denote $\xi(T) = \min\{t \in S_1(T) : g_T(t) \geq 1\}$. Then, we have $g_T(t) < 1$ (i.e., $f(t) < f(t+2)$) for $t = B(T), B(T)+2, \dots, \xi(T)-2$ and $g_T(t) > 1$ (i.e., $f(t) > f(t+2)$) for $t = \xi(T), \xi(T)+2, \dots, F(T)$, so that $\xi(T)$ maximizes $f(t)$ among $t \in S_0(T)$.

B. Proof of Lemma 2

For the cases of $S_1(T) = \emptyset$, $g_T(B(T)) > 1$, or $g_T(F(T)-2) < 1$, similar approach to the proof of Lemma 1 can be applied. All we need to prove is the case of $g_T(B(T)) \leq 1 \leq g_T(F(T)-2)$, which implies $\exists t \in S_1(T)$ such that $g_T(t) = 1$. For this case, denote $\xi(T) = \min\{t \in S_1(T) : g_T(t) \geq 1\}$ and $\eta(T) = \max\{t \in S_1(T) : g_T(t) \leq 1\} + 2$. Based on (13), we have three equations: $f(t) < f(t+2)$ for $t \leq \xi(T)$, $f(t) = f(t+2)$ for $\xi(T)+2 \leq t \leq \eta(T)-2$, and $f(t) > f(t+2)$ for $t \geq \eta(T)$. Therefore, we can conclude that $\forall t \in \{\xi(T), \xi(T)+2, \dots, \eta(T)\}$ maximizes $f(t)$ among $t \in S_1(T)$.

APPENDIX B PROOFS OF PROPOSITIONS 1 AND 2

A. Proof of Proposition 1

Here, we prove that the expression for $\rho(T)$ in (7) coincides with (10) and (11). Note that $S_1(T) = \emptyset$ (i.e., $B(T) = F(T)$) holds if and only if $T = K$ or $T = LK/3$, since we consider the $L \geq 9$ case. We begin with the $S_1(T) = \emptyset$ case, and proceed with the proof for the $S_1(T) \neq \emptyset$ case (i.e., when $T = K+2, K+4, \dots, LK/3-2$).

When $T = K$, $\rho(T) = B(T) = K_1$ from (7), which coincides with $\rho(T) = T - K_2 = K - K_2 = K_1$ in (10) and (11). When $T = LK/3$, $\rho(T) = B(T) = LK_1/3$ from

(7), which coincides with $\rho(T) = LK_1/3$ in (10) and (11). Now we proceed to the case of $K < T < LK/3$.

Case A: if $3^s \geq \frac{L}{3}$

Expressions (7) and (10) are compared. The proof is divided into three cases.

Case A-1 (for $K < T \leq K_2 + \frac{LK_1}{3}$)

$F(T) = T - K_2$ from the definition of $F(T)$. Therefore, all we need to prove is $\rho(T) = F(T)$ for this T interval. Note that $g_T(F(T) - 2) = g_T(T - K_2 - 2) = \frac{1-\omega}{\omega} 3^{\chi(T-K_2-2, K_1)}$. Since $\chi(N_{p0}, K)$ is a monotonically increasing function of N_{p0} , we have $g_T(F(T) - 2) \leq \frac{1-\omega}{\omega} 3^{\chi(LK_1/3-2, K_1)} < 3^{-(s-1)} \frac{L}{9} \leq 1$ holds for $K < T \leq K_2 + \frac{LK_1}{3}$. Therefore, from (7), $g_T(F(T) - 2) < 1$ implies $\rho(T) = F(T)$, which completes the proof.

Case A-2 (for $K_2 + \frac{LK_1}{3} < T < \frac{LK}{3}$)

From case A-1, we have $g_T(F(T) - 2) < 1$ for $T = K_2 + LK_1/3$. Also, from the definition of $F(T)$, we have $F(T + 2) = F(T) = LK_1/3$ for $K_2 + LK_1/3 \leq T < LK/3$. Thus, $g_{T+2}(F(T+2) - 2) = g_{T+2}(F(T) - 2) \leq g_T(F(T) - 2) < 1$. In summary, $g_T(F(T) - 2) < 1$ holds for $K_2 + \frac{LK_1}{3} < T < \frac{LK}{3}$, which implies $\rho(T) = F(T)$ from (7). Using $F(T) = LK_1/3$ for given range of T , we can confirm (7) coincides with (10).

Case B: if $3^s < \frac{L}{3}$

Expressions (7) and (11) are compared. The proof is divided into three cases.

Case B-1 (for $K < T \leq K_2 + 3^s K_1$)

Taking similar approach to case A-1 results in $\rho(T) = F(T) = T - K_2$ for these T values.

Case B-2 (for $K_2 + 3^s K_1 < T < \frac{LK_1}{3} + \frac{LK_2}{3^{s+1}}$)

Denote $\xi(T) = \min\{t \in S_1(T) \mid g_T(t) \geq 1\}$. The proof is divided into two parts: we first prove $g_T(B(T)) \leq 1 \leq g_T(F(T) - 2)$ and then prove $\xi(T) = \phi(T)$ for a given T range. First, recall $B(T) = \max(K_1, T - LK_2/3)$. If $B(T) = K_1$, then

$$\begin{aligned} g_T(B(T)) &= 3^{-\chi(T-K_1-2, K_2)} \frac{1-\omega}{\omega} \\ &< 3^{-\chi(K_2+3^s K_1-K_1-2, K_2)} \frac{1-\omega}{\omega} \leq \frac{1-\omega}{\omega} \leq 1 \end{aligned}$$

since χ is a nonnegative-valued function. If $B(T) = T - \frac{LK_2}{3}$, then

$$g_T(B(T)) = 3^{\chi(T-\frac{LK_2}{3}, K_1) - \chi(\frac{LK_2}{3}-2, K_2)} \frac{1-\omega}{\omega} \leq 1$$

since $T < LK/3$. Similarly, recall $F(T) = \min(T - K_2, \frac{LK_1}{3})$. If $F(T) = T - K_2$, then

$$\begin{aligned} g_T(F(T) - 2) &= 3^{\chi(T-K_2-2, K_1) - \chi(K_2, K_2)} \frac{1-\omega}{\omega} \\ &\geq 3^{\chi(3^s K_1, K_1) - \chi(K_2, K_2)} \frac{1-\omega}{\omega} = 3^s \frac{1-\omega}{\omega} \geq 1 \end{aligned}$$

since $T \geq K_2 + 3^s K_1 + 2$. If $F(T) = \frac{LK_1}{3}$, then

$$\begin{aligned} g_T(F(T) - 2) &= 3^{\chi(\frac{LK_1}{3}-2, K_1) - \chi(T-\frac{LK_1}{3}, K_2)} \frac{1-\omega}{\omega} \\ &= 3^{\log_3 L - 2 - \chi(T-\frac{LK_1}{3}, K_2)} \frac{1-\omega}{\omega} \\ &\geq 3^{\log_3 L - 2 - (\log_3 L - 2 - s)} \frac{1-\omega}{\omega} = 3^s \frac{1-\omega}{\omega} \geq 1 \end{aligned}$$

since $T \leq \frac{LK_1}{3} + \frac{LK_2}{3^{s+1}} - 2$. Thus, we have $g_T(B(T)) \leq 1 \leq g_T(F(T) - 2)$ for given T range.

Now, we just need to prove $\xi(T) = \phi(T)$. We start with proving $\xi(T) = 3^{V(T)+s-1} K_1$ for $T \leq 3^{V(T)+s-1} K_1 + 3^{V(T)} K_2$. First,

$$\begin{aligned} g_T(3^{V(T)+s-1} K_1 - 2) &= 3^{\chi(3^{V(T)+s-1} K_1 - 2, K_1) - \chi(T - 3^{V(T)+s-1} K_1, K_2)} \frac{1-\omega}{\omega} \\ &= 3^{V(T)+s-2 - \chi(T - 3^{V(T)+s-1} K_1, K_2)} \frac{1-\omega}{\omega} \\ &< 3^{V(T)+s-2 - \chi(3^{V(T)-1} K_2, K_2)} \frac{1-\omega}{\omega} \\ &= 3^{V(T)+s-2 - V(T)+1} \frac{1-\omega}{\omega} = 3^{s-1} \frac{1-\omega}{\omega} < 1 \end{aligned}$$

where the first inequality is from $T > 3^{V(T)+s-1} K_1 + 3^{V(T)-1} K_2$ by the definition of $V(T)$. Moreover,

$$\begin{aligned} g_T(3^{V(T)+s-1} K_1) &= 3^{\chi(3^{V(T)+s-1} K_1, K_1) - \chi(T - 3^{V(T)+s-1} K_1 - 2, K_2)} \frac{1-\omega}{\omega} \\ &= 3^{V(T)+s-1 - \chi(T - 3^{V(T)+s-1} K_1 - 2, K_2)} \frac{1-\omega}{\omega} \\ &\geq 3^{V(T)+s-1 - \chi(3^{V(T)} K_2 - 2, K_2)} \frac{1-\omega}{\omega} = 3^s \frac{1-\omega}{\omega} \geq 1 \end{aligned}$$

where the first inequality is from $T \leq 3^{V(T)+s-1} K_1 + 3^{V(T)} K_2$. Therefore, $\xi(T) = \min\{t \in S_1(T) : g_T(t) \geq 1\} = 3^{V(T)+s-1} K_1$.

The next step is to prove $\xi(T) = T - 3^{V(T)} K_2$ for $T > 3^{V(T)+s-1} K_1 + 3^{V(T)} K_2$. First,

$$\begin{aligned} g_T(T - 3^{V(T)} K_2 - 2) &= 3^{\chi(T - 3^{V(T)} K_2 - 2, K_1) - \chi(3^{V(T)} K_2, K_2)} \frac{1-\omega}{\omega} \\ &\leq 3^{\chi(3^{V(T)+s} K_1 - 2, K_1) - V(T)} \frac{1-\omega}{\omega} \leq 3^{s-1} \frac{1-\omega}{\omega} < 1 \end{aligned}$$

where the first inequality is from $T \leq 3^{V(T)+s} K_1 + 3^{V(T)} K_2$ by the definition of $V(T)$. Also,

$$\begin{aligned} g_T(T - 3^{V(T)} K_2) &= 3^{\chi(T - 3^{V(T)} K_2, K_1) - \chi(3^{V(T)} K_2 - 2, K_2)} \frac{1-\omega}{\omega} \\ &= 3^{\chi(T - 3^{V(T)} K_2, K_1) - V(T)+1} \frac{1-\omega}{\omega} \\ &> 3^{\chi(3^{V(T)+s-1} K_1, K_1) - V(T)+1} \frac{1-\omega}{\omega} \\ &= 3^{V(T)+s-1 - V(T)+1} \frac{1-\omega}{\omega} = 3^s \frac{1-\omega}{\omega} \geq 1 \end{aligned}$$

where the first inequality is from $T > 3^{V(T)+s-1} K_1 + 3^{V(T)} K_2$. Therefore, $\xi(T) = \min\{t \in S_1(T) : g_T(t) \geq 1\} = T - 3^{V(T)} K_2$. In summary, $\xi(T) = \phi(T)$ for a given range of T .

Case B-3 (for $\frac{LK_1}{3} + \frac{LK_2}{3^{s+1}} \leq T < \frac{LK}{3}$)

From the definition of $F(T)$, we have $F(T) = \frac{LK_1}{3}$. Therefore, $g_T(F(T) - 2) = 3^{\chi(\frac{LK_1}{3}-2, K_1) - \chi(T-\frac{LK_1}{3}, K_2)} \frac{1-\omega}{\omega} \leq 3^{s-1} \frac{1-\omega}{\omega} < 1$. From (7), we have $\rho(T) = F(T) = \frac{LK_1}{3}$.

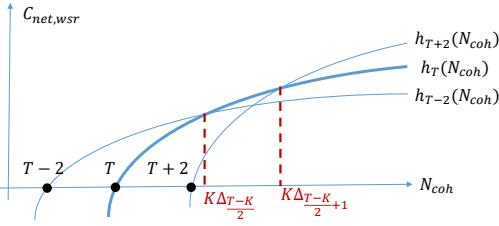


Fig. 7: Graphical explanation for proof of Theorem 2

B. Proof of Proposition 2

Consider $3^s \geq \frac{L}{3}$ case. From Proposition 1, we have $\rho(T+2) = \rho(T) + 2$ for $K \leq T < K_2 + \frac{LK_1}{3}$ and $\rho(T+2) = \rho(T) = \frac{LK_1}{3}$ for $K_2 + \frac{LK_1}{3} \leq T < \frac{LK_1}{3}$. If $3^s < \frac{L}{3}$, from the proposition 1, we have $\rho(T+2) = \rho(T) + 2$ for $K \leq T < K_2 + 3^s K_1$ and $\rho(T+2) = \rho(T) = \frac{LK_1}{3}$ for $\frac{LK_1}{3} + \frac{LK_2}{3^{s+1}} \leq T < \frac{LK_1}{3}$. In case of $K_2 + 3^s K_1 \leq T < \frac{LK_1}{3} + \frac{LK_2}{3^{s+1}}$, we have $\rho(T+2) = \rho(T)$ for $T < 3^{V(T)+s-1} K_1 + 3^{V(T)} K_2$ and $\rho(T+2) = \rho(T) + 2$ for $T \geq 3^{V(T)+s-1} K_1 + 3^{V(T)} K_2$. Therefore, for every case, we have either $\rho(T+2) = \rho(T) + 2$ or $\rho(T+2) = \rho(T)$.

APPENDIX C

PROOF OF COROLLARY 1

We start with the case of $T \geq \frac{LK_1}{3} + \max\{\frac{L}{3^{s+1}}, 1\} K_2$. From Proposition 1, we have $\rho(T+2) = \rho(T) = \frac{LK_1}{3}$ in this T range. Therefore, from Theorem 1, we have $[\mathbf{p}'_{opt,K_1}(\frac{LK_1}{3}), \mathbf{p}'_{opt,K_2}(T - \frac{LK_1}{3})] \in \tilde{P}_{opt}(T)$, which result in $\tilde{C}_{wsr}(T) = \omega C_{sum}(\mathbf{p}'_{opt,K_1}(\frac{LK_1}{3})) + (1 - \omega) C_{sum}(\mathbf{p}'_{opt,K_2}(T - \frac{LK_1}{3}))$. Finally, we obtain $\tilde{C}_{wsr}(T+2) - \tilde{C}_{wsr}(T) = (1 - \omega) C_{sum}(\mathbf{p}'_{opt,K_2}(T+2 - \frac{LK_1}{3})) - (1 - \omega) C_{sum}(\mathbf{p}'_{opt,K_2}(T - \frac{LK_1}{3})) = (1 - \omega) L 3^{-d_2} (C_{d_2+1} - C_{d_2})$ where $d_2 = \chi(T - \rho(T), K_2)$.

In other cases ($T < \frac{LK_1}{3} + \max(\frac{L}{3^{s+1}}, 1) K_2$), we have either $\rho(T+2) = \rho(T)$ or $\rho(T+2) = \rho(T) + 2$ from Proposition 2. Denote $\mathbf{p}_1^* = \mathbf{p}'_{opt,K_1}(\rho(T))$ and $\mathbf{p}_2^* = \mathbf{p}'_{opt,K_2}(T+2 - \rho(T))$. Also, denote $\mathbf{p}_1^{**} = \mathbf{p}'_{opt,K_1}(\rho(T)+2)$ and $\mathbf{p}_2^{**} = \mathbf{p}'_{opt,K_2}(T - \rho(T))$. Then, we can confirm that $[\mathbf{p}_1^*, \mathbf{p}_2^*] \in \Theta(T+2)$ and $[\mathbf{p}_1^{**}, \mathbf{p}_2^{**}] \in \Theta(T+2)$. Since $\tilde{P}_{opt}(T)$ chooses $[\mathbf{p}_1, \mathbf{p}_2] \in \Theta(T)$ which maximizes the WSR, we have $\tilde{C}_{wsr}(T+2) = \max\{C_{wsr}(\mathbf{p}_1^*, \mathbf{p}_2^*), C_{wsr}(\mathbf{p}_1^{**}, \mathbf{p}_2^{**})\}$. Comparing this value with $\tilde{C}_{wsr}(T) = C_{wsr}(\mathbf{p}'_{opt,K_1}(\rho(T)), \mathbf{p}'_{opt,K_2}(T - \rho(T)))$, we have $\tilde{C}_{wsr}(T+2) = \tilde{C}_{wsr}(T) + \delta_T$ where $\delta_T = \max\{(1 - \omega) L 3^{-d_2} (C_{d_2+1} - C_{d_2}), \omega L 3^{-d_1} (C_{d_1+1} - C_{d_1})\}$ (note that d_1 and d_2 are defined in the statement of Corollary 1).

APPENDIX D

PROOF OF THEOREM 2

We wish to find $\mathbf{p}_{opt}(N_{coh})$ that maximizes $C_{net,wsr}$ for any N_{coh} . Since $[\mathbf{p}'_{opt,K_1}(\rho(T)), \mathbf{p}'_{opt,K_2}(T - \rho(T))]$ maximizes C_{wsr} for the given T constraint (from Theorem 1), all we need to compare is $h_T(N_{coh})$ values for different $T \in \{K, K+2, \dots, LK/3\}$. Fig. 7 illustrates the graph of $h_T(N_{coh})$ for three consecutive T values.

We start with checking the N_{coh} value where $h_T(N_{coh})$ and $h_{T+2}(N_{coh})$ crosses. Based on the definition, $h_T(N_{coh}) =$

$h_{T+2}(N_{coh})$ reduces to $N_{coh} = T + 2 + \frac{2\tilde{C}_{wsr}(T)}{\delta_T}$. Similarly, $h_{T-2}(N_{coh})$ and $h_T(N_{coh})$ crosses at $N_{coh} = T + \frac{2\tilde{C}_{wsr}(T-2)}{\delta_{T-2}}$. Therefore, $[\mathbf{p}'_{opt,K_1}(\rho(T)), \mathbf{p}'_{opt,K_2}(T - \rho(T))]$ has maximum $C_{net,wsr}$ for $N_{coh} \in [T + \frac{2\tilde{C}_{wsr}(T-2)}{\delta_{T-2}}, T + 2 + \frac{2\tilde{C}_{wsr}(T)}{\delta_T}]$. For general $T \in \{K, K+2, \dots, LK/3\}$ values, we used sequence Δ_n for the final statement.

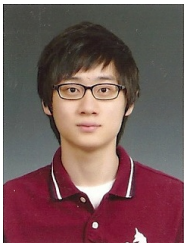
REFERENCES

- [1] T. L. Marzetta, "How much training is required for multiuser mimo?" in *2006 Fortieth Asilomar Conference on Signals, Systems and Computers*. IEEE, 2006, pp. 359–363.
- [2] —, "Noncooperative cellular wireless with unlimited numbers of base station antennas," *IEEE Transactions on Wireless Communications*, vol. 9, no. 11, pp. 3590–3600, 2010.
- [3] L. Lu, G. Y. Li, A. L. Swindlehurst, A. Ashikhmin, and R. Zhang, "An overview of massive mimo: Benefits and challenges," *IEEE Journal of Selected Topics in Signal Processing*, vol. 8, no. 5, pp. 742–758, 2014.
- [4] E. G. Larsson, O. Edfors, F. Tufvesson, and T. L. Marzetta, "Massive mimo for next generation wireless systems," *IEEE Communications Magazine*, vol. 52, no. 2, pp. 186–195, 2014.
- [5] J. G. Andrews, S. Buzzi, W. Choi, S. V. Hanly, A. Lozano, A. C. Soong, and J. C. Zhang, "What will 5g be?" *IEEE Journal on Selected Areas in Communications*, vol. 32, no. 6, pp. 1065–1082, 2014.
- [6] O. Elijah, C. Y. Leow, T. A. Rahman, S. Nunoo, and S. Z. Iliya, "A comprehensive survey of pilot contamination in massive mimo-5g system," *IEEE Communications Surveys & Tutorials*, vol. 18, no. 2, pp. 905–923, 2015.
- [7] K. Appaiah, A. Ashikhmin, and T. L. Marzetta, "Pilot contamination reduction in multi-user tdd systems," in *2010 IEEE International Conference on Communications (ICC)*, pp. 1–5.
- [8] H. Yin, D. Gesbert, M. Filippou, and Y. Liu, "A coordinated approach to channel estimation in large-scale multiple-antenna systems," *IEEE Journal on Selected Areas in Communications*, vol. 31, no. 2, pp. 264–273, 2013.
- [9] J. Jose, A. Ashikhmin, T. L. Marzetta, and S. Vishwanath, "Pilot contamination and precoding in multi-cell tdd systems," *IEEE Transactions on Wireless Communications*, vol. 10, no. 8, pp. 2640–2651, 2011.
- [10] A. Ashikhmin and T. Marzetta, "Pilot contamination precoding in multi-cell large scale antenna systems," in *Information Theory Proceedings (ISIT), 2012 IEEE International Symposium on*, pp. 1137–1141.
- [11] X. Li, E. Bjornson, E. G. Larsson, S. Zhou, and J. Wang, "A multi-cell mmse detector for massive mimo systems and new large system analysis," in *2015 IEEE Global Communications Conference*, pp. 1–6.
- [12] H. Q. Ngo, M. Matthaiou, and E. G. Larsson, "Performance analysis of large scale mu-mimo with optimal linear receivers," in *Communication Technologies Workshop (Swe-CTW), 2012 Swedish*. IEEE, 2012, pp. 59–64.
- [13] K. Guo and G. Ascheid, "Performance analysis of multi-cell mmse based receivers in mu-mimo systems with very large antenna arrays," in *Wireless Communications and Networking Conference (WCNC), 2013 IEEE*, pp. 3175–3179.
- [14] K. Guo, Y. Guo, G. Fodor, and G. Ascheid, "Uplink power control with mmse receiver in multi-cell mu-massive-mimo systems," in *Communications (ICC), 2014 IEEE International Conference on*, pp. 5184–5190.
- [15] X. Zhu, Z. Wang, L. Dai, and C. Qian, "Smart pilot assignment for massive mimo," *IEEE Communications Letters*, vol. 19, no. 9, pp. 1644–1647, 2015.
- [16] T. M. Nguyen, V. N. Ha, and L. B. Le, "Resource allocation optimization in multi-user multi-cell massive mimo networks considering pilot contamination," *IEEE Access*, vol. 3, pp. 1272–1287, 2015.
- [17] B. Liu, Y. Cheng, and X. Yuan, "Pilot contamination elimination precoding in multi-cell massive mimo systems," in *Personal, Indoor, and Mobile Radio Communications (PIMRC), 2015 IEEE 26th Annual International Symposium on*, pp. 320–325.
- [18] E. Björnson, E. G. Larsson, and M. Debbah, "Massive mimo for maximal spectral efficiency: How many users and pilots should be allocated?" *IEEE Transactions on Wireless Communications*, vol. 15, no. 2, pp. 1293–1308, 2016.
- [19] V. Saxena, G. Fodor, and E. Karipidis, "Mitigating pilot contamination by pilot reuse and power control schemes for massive mimo systems," in *2015 IEEE 81st Vehicular Technology Conference (VTC Spring)*. IEEE, 2015, pp. 1–6.

- [20] J. Y. Sohn, S. W. Yoon, and J. Moon, "When pilots should not be reused across interfering cells in massive mimo," in *2015 IEEE International Conference on Communication Workshop (ICCW)*. IEEE, 2015, pp. 1257–1263.
- [21] X. Gao, O. Edfors, F. Rusek, and F. Tufvesson, "Massive mimo performance evaluation based on measured propagation data," *IEEE Transactions on Wireless Communications*, vol. 14, no. 7, pp. 3899–3911, 2015.



Jy-yong Sohn received the B.S. and M.S. degrees in electrical engineering from the Korea Advanced Institute of Science and Technology (KAIST), Daejeon, Korea, in 2014 and 2016, respectively. He is currently pursuing the Ph.D. degree in KAIST. His research interests include massive MIMO effects on wireless multi cellular system and 5G Communications, with a current focus on distributed storage and network coding.



Sung Whan Yoon received the B.S. and M.S. degrees in electrical engineering from the Korea Advanced Institute of Science and Technology (KAIST), Daejeon, Korea, in 2011 and 2013, respectively. He is currently pursuing the Ph.D degree in KAIST. His main research interests are in the field of coding and signal processing for wireless communication & storage, especially massive MIMO, polar codes and distributed storage codes.



Jaekyun Moon received the Ph.D degree in electrical and computer engineering at Carnegie Mellon University, Pittsburgh, Pa, USA. He is currently a Professor of electrical engineering at KAIST. From 1990 through early 2009, he was with the faculty of the Department of Electrical and Computer Engineering at the University of Minnesota, Twin Cities. He consulted as Chief Scientist for DSPG, Inc. from 2004 to 2007. He also worked as Chief Technology Officer at Link-A-Media Devices Corporation. His research interests are in the area of channel

characterization, signal processing and coding for data storage and digital communication. Prof. Moon received the McKnight Land-Grant Professorship from the University of Minnesota. He received the IBM Faculty Development Awards as well as the IBM Partnership Awards. He was awarded the National Storage Industry Consortium (NSIC) Technical Achievement Award for the invention of the maximum transition run (MTR) code, a widely used error-control/modulation code in commercial storage systems. He served as Program Chair for the 1997 IEEE Magnetic Recording Conference. He is also Past Chair of the Signal Processing for Storage Technical Committee of the IEEE Communications Society. In 2001, he cofounded Bermat, Inc., a fabless semiconductor start-up, and served as founding President and CTO. He served as a guest editor for the 2001 IEEE JSAC issue on Signal Processing for High Density Recording. He also served as an Editor for IEEE TRANSACTIONS ON MAGNETICS in the area of signal processing and coding for 2001-2006. He is an IEEE Fellow.